# Blue Electrophosphorescence from Iridium Complex Covalently Bonded to the Poly(9-dodecyl-3-vinylcarbazole): Suppressed Phase Segregation and Enhanced Energy Transfer

**Youngmin You,[†] Se Hun Kim,[‡] Ho Kuk Jung,[†] and Soo Young Park*,[†]**

*School of Materials Science & Engineering, Seoul National University, San 56-1, Shillim-Dong, Kwanak-Gu, Seoul 151-744, Korea, and Central R&D Center, Dongwoo FineChem Co., Ltd.,1177, Pyungtaek-Si, Kyunggi-Do 451-764, Korea*

*Received September 15, 2005; Revised Manuscript Received November 7, 2005*

ABSTRACT: Efficient blue electrophosphorescence was achieved from iridium(III) bis[(4,6-difluorophenyl)-pyridinato-*N*,$C^{2'}$]picolinate (FIrpic) covalently bonded to the carbazole-based wide-band-gap polymer host (poly-(9-dodecyl-3-vinylcarbazole); $CP_0$). Number-average molecular weights of $CP_0$-based copolymers containing FIrpic pendants ($CP_n$) ranged over 18 000−33 700 when the molar content of FIrpic-containing monomer units was 0.8−10.6%: $CP_1$ (0.8%), $CP_2$ (2.9%), $CP_3$ (5.3%), and $CP_4$ (10.6%). Phase segregation in the $CP_n$ copolymer was significantly suppressed compared to that in the doped analogues (molecular composite of $CP_0$/FIrpic). The photoluminescence spectra of the carbazole-based polymer host ($CP_0$) overlapped with the absorption band of FIrpic, and the $T_1$ level of $CP_0$ (−2.6 eV) was higher than that of FIrpic (−3.1 eV), ensuring highly efficient exothermic energy transfer. Electroluminescence (EL) devices employing $CP_n$ polymers as emitting layer showed exclusive FIrpic emission due to the efficient energy transfer and subsequent exciton confinement in FIpic. The luminance of preliminary EL devices reached as high as 1450 cd/m$^2$ with emission efficiency of 2.23 cd/A. It was specifically noted that the roll-off of external quantum efficiency in the region of high current density was interestingly suppressed in the $CP_n$ polymer devices.

## Introduction

Phosphorescent organic light emitting diode (OLED) utilizing iridium(III) complex is gaining ever increasing attention due to its much higher external quantum efficiency than that of fluorescent OLED. Strong spin−orbit coupling in the iridium-(III) complex provides relatively shorter lifetime of triplet metal-to-ligand charge-transfer (MLCT) state, which allows efficient utilization of triplet excitons in addition to the singlet excitons to achieve nearly 100% internal quantum efficiency of the electroluminescence device.[1,2]

In a phosphorescent OLED, a host−guest system is largely empolyed in order to prevent destructive excited-state interactions between emitting phosphors, like triplet−triplet annihilation, especially under high current density.[3] Normally, phosphorescent emitting layers comprise molecular[4,5] or polymeric[6−9] hosts doped by small amount of phosphorescent iridium(III) complex, which unfortunately does not guarantee fine dispersion of highly crystalline dopants in a host matrix.[10] Such an inherent phase segregation in a host−guest system brings about excited-state interchromophoric interactions yielding low device efficiency.[10] Therefore, a polymeric host with covalently bonded phosphorescent chromophores has been regarded as the viable solution with additional benefits of excellent processability and stability.

In this sense, polyfluorenes side-chained by green and red emitting iridium(III) complexes have already been reported.[11,12] However, for the blue phosphorescence, polyfluorene and other conjugated polymers are not the proper hosts due to their relatively lower $T_1$ level which does not ensure exothermic energy transfer to the blue emitting side-chain guest.[13]

Nonconjugated carbazole-based polymer, on the other hand, seems to be one of the most promising hosts for blue phosphors because the excited-state energy level ($S_1 = -2.2$, $T_1 = -2.6$ eV) and $S_0$ level (−5.8 eV) of carbazole match well those of FIrpic ($T_1 = -3.1$, $S_0 = -5.7$ eV), a widely used blue phosphor, for the exothermic energy transfer. Poly(vinylcarbazole) (PVK) is the most representative and well-known polymer among carbazole-based polymers.[14−17] Unfortunately, PVK features a strong tendency of excimer formation with its triplet emission longer than 502 nm, which limits the efficient hosting of 480 nm emitting FIrpic. To be a proper host of blue emitting FIrpic, therefore, some structural modifications on the carbazole-based polymer to reduce the excimer formation are demanded. In this paper, we investigated a novel carbazole-based polymer (poly-(9-dodecyl-3-vinylcarbazole), $CP_0$) and its copolymers ($CP_n$) containing covalently bonded FIrpic pendant, which successfully showed reduced excimer formation and efficient excites-state energy transfer (see Chart 1 for the polymer structure).

Important issues covered in this work include (a) suppressed phase segregation in $CP_n$ compared to the doped analogue (molecular composite of FIrpic in $CP_0$), (b) identification of excited-state energy transfer from polymer host to the tethered FIrpic unit, and (c) the electroluminescence characteristics.

## Experimental Section

**Synthesis.** Tetrahydrofuran (THF) was distilled with sodium and benzophenone under a nitrogen atmosphere before use. Commercial TLC plates (silica gel 60 $F_{254}$, Merck Co.) were used to monitor the progress of the reaction, with spots observed under UV light at 254 and 365 nm or stained with *p*-anisaldehyde. Silica column chromatography was performed with silica gel 60 G (particle size 5−40 $\mu$m, Merck Co.). Unless otherwise mentioned, materials obtained from commercial supplier were used without additional purification.

**Methyl-3-hydroxypicolinate.** After dissolving 3-hydroxypicolinic acid (2.00 g, 14.4 mmol) in methanol (200 mL), sulfuric acid (4 mL) was added dropwise to the reaction mixture. Refluxing

[†] Seoul National University.
[‡] Dongwoo FineChem Co., Ltd.

10.1021/ma052015t CCC: $33.50 
Published on Web 12/09/2005

**Chart 1. Structure of Polymers**

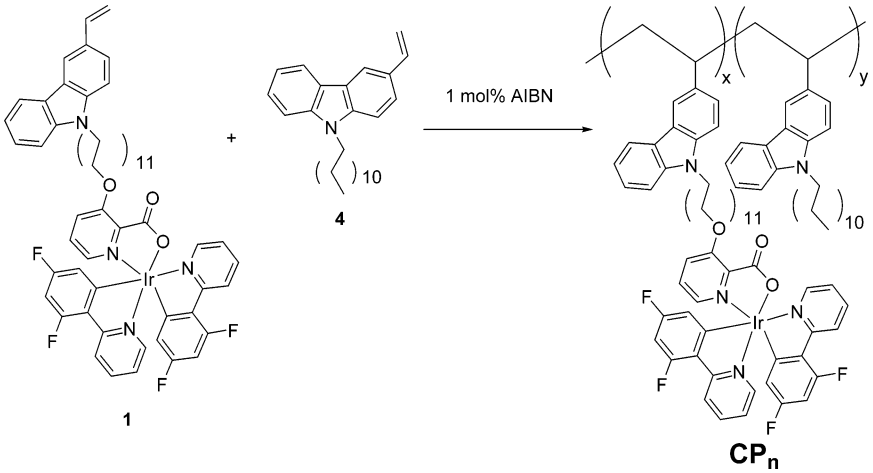


for 1 day gave dark brown solution which was cooled to room temperature and poured into water. Neutralization with saturated aqueous sodium bicarbonate to pH 6 followed by extraction with dichloromethane ($CH_2Cl_2$) (100 mL × 3) was performed. The obtained organic layer was dried over anhydrous magnesium sulfate and concentrated. Silica column purification (*n*-hexane:ethyl acetate (EtOAc) = 1:3) was carried out to give white powder (1.85 g, 12.1 mmol) in 84% yield. TLC, $R_f$ = 0.1 (*n*-hexane:$CH_2Cl_2$ = 1:1). $^1$H NMR $\delta$: 4.07 (s, 3H), 7.37 (d, $J$ = 1.7), 7.40 (d, $J$ = 1.7), 7.43 (d, $J$ = 4.2), 7.46 (d, $J$ = 4.4), 8.29 (dd, $J$ = 4.0, 1.7, 1H), 10.7 (s, 1H). $^{13}$C NMR (125 MHz) $\delta$: 53.3, 126.4, 129.8, 130.2, 141.7, 159.0, 170.0. HRMS (EI): calculated $M^+$ 153.0425; observed $M^+$ 153.0426.

**9-Dodecylcarbazole (2).** To a stirred suspension of potassium hydroxide (2.01 g, 35.9 mmol) in *N*,*N*-dimethylformaide (DMF) (100 mL), carbazole (3.00 g, 17.9 mmol) was added and stirred. After 1 h 1-dodecyl bromide was delivered via pipet, and the solution was further stirred for 6 h. The reaction mixture was poured into brine and extracted with ethyl acetate (100 mL × 2). The organic layer was washed with water (100 mL × 2) and dried over anhydrous magnesium sulfate. Evaporation of solvents in a rotary evaporator and silica column purification (*n*-hexane:$CH_2Cl_2$ = 4:1) gave a transparent sticky liquid (6.01 g, 17.9 mmol) in 99% yield. TLC, $R_f$ = 0.5 (*n*-hexane:$CH_2Cl_2$ = 7:3). $^1$H NMR (500 MHz) $\delta$: 0.99 (m, 3H), 1.33 (br, 20H), 1.94 (m, 2H), 4.34 (t, $J$ = 7.3, 2H), 7.32 (t, $J$ = 7.6, 2H), 7.48 (d, $J$ = 8.2, 2H), 7.55 (t, $J$ = 7.4, 2H), 8.19 (d, $J$ = 7.8, 2H). $^{13}$C NMR (125 MHz) $\delta$: 14.3, 22.9, 27.5, 29.2, 29.6, 29.7, 29.8, 32.1, 43.2, 108.8, 118.9, 120.5, 123.0, 125.7, 140.6. HRMS (EI): calculated $M^+$ 335.2612; observed $M^+$ 335.2613.

**9-Dodecyl-3-formylcarbazole (3).** To a stirred solution of DMF (1.02 mL, 45.8 mmol) in the ice bath, phosphorus oxychloride (2.85 mL, 30.5 mmol) was added via syringe under a nitrogen atmosphere. After 1 h the reaction vessel was warmed to room temperature, and 9-dodecylcarbazole (**2**) (5.12 g, 15.3 mmol) dissolved in DMF (10 mL) was added to the reaction mixture. Then the reaction temperature was raised to 110 °C. After 1 day, the reaction mixture was poured into cooled aqueous sodium bicarbonate solution and extracted with ethyl acetate (100 mL). Residual DMF was removed via repetitive extraction with water (100 mL × 3). The organic layer was dried over anhydrous magnesium sulfate and concentrated. Silica column purification gave a yellow powder (4.89 g, 13.5 mmol) in 88% yield. TLC, $R_f$ = 0.2 (*n*-hexane:$CH_2Cl_2$ = 1:1). $^1$H NMR (500 MHz) $\delta$: 0.87 (t, $J$ = 6.8, 3H), 1.23 (br, 20H), 2.04 (m, 2H), 4.32 (t, $J$ = 7.3, 2H), 7.32 (t, $J$ = 7.2, 1H), 7.45 (d, $J$ = 7.4, 1H), 7.47 (d, $J$ = 8.2, 1H), 8.00 (d, $J$ = 8.6, 1H), 8.15 (d, $J$ = 7.7, 1H), 8.60 (s, 1H), 10.90 (s, 1H). $^{13}$C NMR (125 MHz) $\delta$: 14.2, 22.8, 27.4, 29.0, 29.4, 29.5, 29.6, 29.7, 32.0, 43.5, 109.0, 109.5, 120.4, 120.8, 123.1, 124.1, 126.8, 127.3, 128.6, 141.3, 144.2, 191.9. HRMS (EI): calculated $M^+$ 363.2566; observed $M^+$ 363.2562.

**9-Dodecyl-3-vinylcarbazole (4).** 9-Dodecyl-3-formylcarbazole (**3**) (3.00 g, 8.25 mmol), methyltriphenylphosphonium bromide (8.84 g, 24.8 mmol), and potassium carbonate (3.42 g, 24.8 mmol) were dissolved in 120 mL of 1,4-dioxane. 10 mL of water was added to reaction vessel, and the mixture was refluxed for 3 days. After cooling to room temperature, the reaction mixture was washed with water (100 mL × 3). The crude product was obtained via extraction with ethyl acetate (100 mL) and dried over anhydrous magnesium sulfate. Silica column purification on the concentrate gave a white solid (2.50 g, 6.91 mmol) in 84% yield. TLC, $R_f$ = 0.6 (*n*-hexane:EtOAc = 7:3). $^1$H NMR (500 MHz) $\delta$: 0.91 (t, $J$ = 6.8, 3H), 1.20 (br, 20H), 1.88 (m, 2H), 4.30 (t, $J$ = 7.2, 2H), 5.22 (d, $J$ = 11.0, 1H), 5.80 (d, $J$ = 17.5, 1H), 6.94 (dd, $J$ = 17.5, 10.9, 1H), 7.25 (t, $J$ = 7.2, 1H), 7.36 (d, $J$ = 8.5, 1H), 7.41 (d, $J$ = 8.2, 1H), 7.47 (t, $J$ = 7.1, 1H), 7.60 (d, $J$ = 8.5, 1H), 8.12 (d, $J$ = 7.7, 1H), 8.14 (s, 1H). $^{13}$C NMR (125 MHz) $\delta$: 14.3, 22.9, 27.5, 29.2, 29.5, 29.6, 29.7, 29.8, 32.1, 43.4, 108.9, 109.0, 111.1, 1118.6, 119.1, 120.6, 123.1, 123.2, 124.2, 125.9, 129.0, 137.8, 140.5, 141.0. HRMS (EI): calculated $M^+$ 361.2770; observed $M^+$ 361.2769.

**9-(12-Bromododecyl)carbazole (5).** A magnetically stirred suspension of carbazole (4.00 g, 23.9 mmol) and KOH (2.69 g, 47.8 mmol) in DMF (80 mL) was added to a solution of 1,12-dibromododecane (11.8 g, 35.9 mmol) in DMF (80 mL) via dropping funnel. After 12 h, the reaction mixture was neutralized with saturated aqueous ammonium chloride (150 mL) and then extracted with ethyl acetate (150 mL). The organic layer was washed with water (100 mL × 3) dried over anhydrous magnesium sulfate and concentrated in a rotary evaporator. The crude product was purified with silica column chromatography (*n*-hexane:EtOAc = 50:1) to give sticky brown oil (6.15 g, 14.8 mmol) in 62% yield. TLC, $R_f$ = 0.6 (*n*-hexane:$CH_2Cl_2$ = 1:1). $^1$H NMR $\delta$: 0.88 (t, $J$ = 6.2, 3H), 1.25 (br, 20H), 1.84 (m, 2H), 3.40 (t, $J$ = 6.8, 2H), 4.30 (t, $J$ = 7.3, 2H), 7.23 (m, 4H), 7.42 (m, 4H), 8.10 (d, $J$ = 7.4, 2H).

**3-Bromo-9-(12-bromododecyl)carbazole (6).** To a magnetically stirred solution of 9-(12-bromododecyl)cabazole (**5**) (1.39 g, 3.35 mmol) in THF (40 mL), *N*-bromosuccinimide (NBS) (0.627 g, 3.52 mmol) was added slowly for 10 min. The reaction vessel was shielded from the external light by an aluminum foil and kept being stirred overnight. Then, the reaction mixture was poured into brine and extracted with $CH_2Cl_2$ (100 mL × 2). The extracted organic layer was dried over anhydrous magnesium sulfate and concentrated with a rotary evaporator. The obtained concentrate was purified with silica column chromatography (*n*-hexane:EtOAc = 30:1) to give dark brown solid (1.52 g, 3.07 mmol) in 92% yield. TLC, $R_f$ = 0.3 (*n*-hexane only). $^1$H NMR $\delta$: 0.91 (t, $J$ = 7.1, 3H), 1.25 (br, 20H), 3.40 (t, $J$ = 6.8, 2H), 4.26 (t, $J$ = 7.3, 2H), 7.26 (m, 2H), 7.39 (d, $J$ = 8.1, 1H), 7.49 (m, 2H), 8.04 (d, $J$ = 7.6, 1H), 8.20 (d, $J$ = 1.8, 1H). $^{13}$C NMR (125 MHz) $\delta$: 27.5, 28.4, 28.9, 29.1, 29.5, 29.6, 29.7, 33.0, 34.3, 43.4, 43.6, 109.1, 110.3, 119.4, 120.7, 123.3, 126.5, 128.4, 129.2, 139.3, 140.9.

**Methyl-3-(9-(3-bromocarbazolyl)dodecyl)oxypicolinate (7).** After dispersing KOH (0.254 g, 3.62 mmol) in DMF (80 mL) for 10 min, methyl-3-hydroxypicolinate (0.554 g, 3.62 mmol) was added and kept being stirred for 1 h. Then 3-bromo-9-(12-

bromododecyl)cabazole (**6**) (1.49 g, 3.02 mmol) was delivered, and the reaction vessel was stirred for 1 day. Neutralization with saturated aqueous ammonium chloride (100 mL) followed by extraction with ethyl acetate (100 mL) was performed, and the organic layer was washed with water (100 mL × 2) and then dried over anhydrous magnesium sulfate. The concentrated crude product was purified with silica column chromatography to give a brown sticky solid (1.70 g, 3.00 mmol) in quantitative yield. TLC, $R_f$ = 0.4 (*n*-hexane:EtOAc = 1:1). $^1$H NMR $\delta$: 0.90 (t, $J$ = 7.1, 3H), 1.25 (br, 20H), 4.04 (t, $J$ = 6.6, 2H), 4.27 (t, $J$ = 7.3, 2H), 7.23 (m, 1H), 7.25 (m, 1H), 7.29 (m, 1H), 7.31 (d, $J$ = 1.46), 7.33 (d, $J$ = 1.47), 7.36 (d, $J$ = 4.2), 7.38 (s), 7.41 (s), 7.47 (dd, $J$ = 7.1, 1.3, 1H), 7.53 (d, $J$ = 2.0, 1H), 8.04 (d, $J$ = 7.9, 1H), 8.20 (d, $J$ = 1.8, 1H), 8.25 (dd, $J$ = 4.4, 1.5, 1H). $^{13}$C NMR (75 MHz) $\delta$: 25.8, 27.2, 28.9, 29.2, 29.4, 29.5, 43.2, 52.8, 69.9, 108.9, 110.1, 110.4, 111.5, 119.2, 120.5, 121.8, 122,8, 124.5, 126.3, 127.6, 128.2, 129.0, 139.1, 139.5, 140.7, 155.5, 163.7. HRMS (FAB): calculated $M^+$ 565.2066; observed $M^+$ 565.2061.

**Methyl-3-(9-(3-vinylcarbazolyl)dodecyl)oxypicolinate (8).** Methyl-3-(9-(3-bromocarbazolyl)dodecyl)oxypicolinate (**7**) (1.58 g, 2.79 mmol), tributylvinyltin (4.42 g, 13.9 mmol), and tetrakis(triphenylphosphine)palladium(0) (0.323 g, 0.279 mmol) were stirred for 10 min in toluene under nitrogen atmosphere, and the temperature was raised to 110 °C. After 3 days, the reaction mixture was poured into brine and extracted with ethyl acetate (100 mL). The organic layer was washed with water (100 mL × 3), then dried over anhydrous magnesium sulfate, and concentrated. Further purification of obtained concentrate was done via silica column purification (*n*-hexane:EtOAc = 2:1) to give a brown sticky solid (0.452 g, 0.882 mmol) in 32% yield. TLC, $R_f$ = 0.4 (*n*-hexane:EtOAc = 1:2). $^1$H NMR $\delta$: 0.92 (t, $J$ = 7.1, 3H), 1.27 (br, 20H), 1.57 (s, 2H), 1.59 (s, 2H), 3.96 (s, 3H), 4.04 (t, $J$ = 6.6, 2H), 4.28 (t, $J$ = 7.1, 2H), 5.19 (dd, $J$ = 10.8, 0.9, 1H), 4.04 (t, $J$ = 6.6, 2H), 5.77 (dd, $J$ = 17.5, 0.9, 1H), 6.91 (dd, $J$ = 17.5, 10.8, 1H), 7.23 (m, 2H), 7.30−7.56 (m, 6H), 7.58 (dd, $J$ = 8.5, 1.8, 1H), 8.09 (s, 1H), 8.11 (s, 1H), 8.26 (dd, $J$ = 4.3, 1.3, 1H). HRMS (FAB): calculated $M^+$ 513.3117; observed $M^+$ 513.3117.

**2-(2,4-Difluorophenyl)pyridine (dfppy).** 2-Bromopyridine (2.01 mL, 21.1 mmol), 2,4-difluorophenylboronic acid (4.00 g, 25.3 mmol), and tetrakis(triphenylphosphine)palladium(0) (0.732 g, 0.633 mmol) were added to a round-bottomed flask with reflux condenser and dissolved in 50 mL of THF. After adding 30 mL of aqueous 2 N $Na_2CO_3$, reaction mixture was heated at 70 °C for 1 day. The cooled crude mixture was poured into water and extracted with $CH_2Cl_2$ (50 mL × 3) and then dried over anhydrous magnesium sulfate. Silica column purification (*n*-hexane:EtOAc = 5:1) gave a transparent liquid (4.07 g, 21.0 mmol) in quantitative yield. TLC, $R_f$ = 0.5 (*n*-hexane:EtOAc = 5:1). $^1$H NMR $\delta$: 6.89 (m, 1H), 7.1 (m, 1H), 7.28 (m, 1H), 7.75 (m, 2H), 8.00 (m, 1H), 8.71 (d, $J$ = 3.5, 1H). HRMS (EI): calculated $M^+$ 191.0544; observed $M^+$ 191.0546.

**[(dfppy)$_2$Ir($\mu$-Cl)]$_2$.** $IrCl_3 \cdot H_2O \cdot HCl$ (Aldrich) (0.702 g, 2.35 mmol) and dfppy (2.00 g, 10.5 mmol) were dissolved in 2-ethoxyethanol:water = 60 mL:20 mL and refluxed at 140 °C for 20 h under a nitrogen atmosphere. After cooling, a yellow precipitate was filtered and washed with acetone:ethanol = 60 mL:60 mL. The washed product was recrystallized in *n*-hexane:toluene = 10 mL:25 mL to give yellow crystals (2.28 g, 1.88 mmol) in 85% yield. HRMS (FAB): calculated $M^+$ 1216.0509; observed $M^+$ 1216.0499.

**FIrpicDodCbz (1).** Methyl-3-(9-(3-vinylcarbazolyl)dodecyl)-oxypicolinate (**8**) (0.252 g, 0.491 mmol) and sodium carbonate (0.156 g, 1.47 mmol) were added to 70 mL of methanol. When the reactants were fully dissolved, 10 mL of water was added to reaction vessel under a nitrogen atmosphere with raising the temperature up to 50 °C. The reaction vessel was shielded from the external light with an aluminum foil during the reaction. After 12 h reaction mixture was poured into water, and the solution was adjusted to pH 2 with aqueous 1 N HCl. The crude product was recovered via extraction with ethyl acetate (100 mL × 2) and dried over anhydrous magnesium sulfate. The final acid was purified with silica column purification (EtOAc only). TLC, $R_f$ = 0.4 (EtOAc:MeOH = 9:1). The thoroughly dried acid (0.273 g, 0.547 mmol) and [(dfppy)$_2$Ir($\mu$-Cl)]$_2$ (0.333 g, 0.274 mmol) was dissolved in 2-ethoxyethanol and degassed, and then 1.23 mL of aqueous 2 N NaOH was added to the light-shielded reaction mixture under a nitrogen atmosphere and stirred for 12 h. To remove 2-ethoxyethanol and residual salts, the reaction mixture was washed with water (100 mL × 3) and extracted by EtOAc. The organic layer was dried over anhydrous magnesium sulfate and concentrated. Silica column purification (EtOAc only) gave a faint brown powder (0.536 g, 0.501 mmol) in 91% in two steps. TLC, $R_f$ = 0.6 (EtOAc only). $^1$H NMR $\delta$: 1.23 (br, 20H), 2.02 (s, 4H), 3.47 (dd, $J$ = 14.0, 7.1, 2H), 4.00 (m, 2H), 4.11 (t, $J$ = 7.1, 2H), 4.28 (t, $J$ = 7.0, 2H), 5.19 (d, $J$ = 11.0, 1H), 5.52 (d, $J$ = 8.8, 1H), 5.78 (m, 1H), 6.40 (m, 2H), 6.96 (m, 2H), 7.22 (m, 5H), 7.33−7.27 (m, 7H), 7.57 (d, $J$ = 8.4, 1H), 7.75 (t, $J$ = 7.3, 2H), 8.11 (m, 2H), 8.21 (m, 3H), 8.80 (d, $J$ = 5.0, 1H). Anal. Calcd for $C_{54}H_{49}F_4IrN_4O_3$: C, 57.26; H, 4.59; N, 4.91. Found: C, 56.98; H, 4.56; N, 4.71. HRMS (FAB): calculated $M^+$ 1071.3453; observed $M^+$ 1071.3448.

**Polymerization.** Polymers ($CP_0$, $CP_1$, $CP_2$, $CP_3$, and $CP_4$) were synthesized by free radical copolymerization of **1** and **4**.

**$CP_0$.** 0.500 g of **4** was delivered to a precleaned glass ampule. 2.00 mL solution of 1-methyl-2-pyrrolidinone (NMP) containing 5.0 mg of 2,2′-azobis(isobutyronitrile) (AIBN) was added to the ampule with a micropipet, and the solution was degassed by the standard vacuum−freeze−thaw technique. After sealing the degassed ampule, the solution was heated at 65 °C for 1 day. After cooling to room temperature, the reaction mixture was poured into the stirred metanol and the precipitates were filtered and collected by $CH_2Cl_2$. The concentrated polymer solution in $CH_2Cl_2$ was reprecipitated with MeOH. This procedure was repeated three times to give white powder (0.406 g) in 81% yield.

**$CP_1$.** 12.4 mg of **1** and 0.399 g of **4** were charged to a precleaned glass ampule. A 1.50 mL aliquot from 10.0 mL of NMP master solution containing 18.1 mg of AIBN was added to the ampule with micropipet, and the solution was degassed by the standard vacuum−freeze−thaw technique. After sealing the degassed ampule, the solution was heated at 65 °C for 1 day. The same purification procedure as for $CP_0$ was applied to give a yellow powder (0.124 g) in 67% yield. The comonomer composition of obtained copolymer was analyzed by absorption spectroscopy.

**$CP_2$.** 16.7 mg of **1** and 0.168 g of **4** were dissolved by 1.25 mL solution from 10.0 mL of NMP containing 7.6 mg of AIBN. Polymerization and purification were carried out similarly as for $CP_1$. The final product was obtained as a yellow powder (0.271 g) in 66% yield.

**$CP_3$.** 70.0 mg of **1** and 0.162 g of **4** were dissolved by 1.00 mL solution from 10.0 mL of NMP containing 7.6 mg of AIBN. Polymerization and purification were carried out similarly as for $CP_1$. The final product was obtained as yellow powder (0.144 g) in 62% yield.

**$CP_4$.** 80.0 mg of **1** and 96.8 mg of **4** were dissolved by 1.00 mL solution from 10.0 mL of NMP containing 4.4 mg of AIBN. Polymerization and purification were carried out similarly as for $CP_1$. The final product was obtained as yellow powder (0.113 g) in 64% yield.

**Characterization.** $^1$H and $^{13}$C nuclear magnetic resonance (NMR) spectra were obtained in $CDCl_3$ at 300 MHz (JEOL, JNM-LA 300 or Bruker, Avance DPX-300). Chemical shifts were recorded by ppm. Multiplicity was denoted by s (singlet), d (doublet), t (triplet), dd (doublet of doublet), br (broad), and m (multiplet). Coupling constants ($J$) were in hertz (Hz). Mass spectra (MS) were obtained with HP 3890 series GC system with HP 5973 mass selective detector for low-resolution data, and JEOL, JMS-AX505WA, and HP 5890 series II were used for low-resolution mass spectra using the direct insertion probes (DIP) method and high-resolution mass spectra, respectively. Elemental analysis (EA) was performed with CE Instrument, EA1110. Absorption spectra of polymer solution and film (spin-coated film on precleaned glass substrate under 2500 rpm with 1.7 wt % solution in 1,2-dichloroethane) were recorded with a Shimazu UV-1650PC from

**Scheme 1. Synthesis of 9-Dodecyl-3-vinylcarbazole (4)**

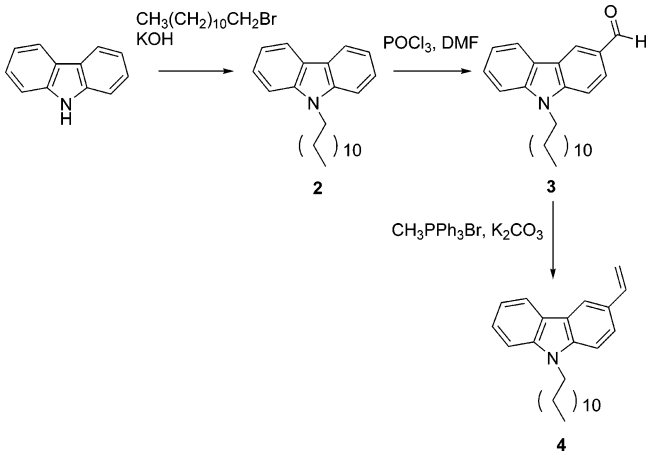


220 to 650 nm with 0.2 nm increments. Photoluminescence spectra were obtained with a Shimazu RF 5301 PC spectrophotometer. Gel permeation chromatographic (GPC) measurements were taken in a system comprising P1000, Rheodyne 7725i, T60, LR40, and Trisec polystyrene as a standard. Differential scanning calorimetry (DSC) was carried out under a nitrogen atmosphere at a heating rate of 20 °C/min on a Perkin-Elmer DSC7. Time-resolved photoluminescence spectra were measured in a time window of 0−30 ms with a Hamamatsu R5509 PMT through monochromator. The polymer film loaded inside a cryostat was cooled to 7 K by a flowing helium gas via a closed cycle cryogenic system. The fourth harmonics of a Q-switched Nd:YAG laser with pulse duration of 6 ns, repetition rate of 10 Hz, and optical power of ∼50 mJ was loosely focused on the sample within the diameter of 10 mm. Confocal laser scanning microscope (CLSM, 25 mW of Ar laser) images of polymer films on glass were taken with Carl Zeiss-LSM510. Cyclic voltametric experiments were carried out with a model 273A (Princeton Applied Research) using an one-compartment electrolysis cell consisting of a platinum working electrode, a platinum wire counter electrode, and a quasi $Ag^+/Ag$ reference electrode. The measurements were done in 0.5 mM $CH_2Cl_2$ solution with tetrabutylammonium tetrafluoroborate as supporting electrolyte at a scan rate of 50 mV/s. Each oxidation potential was calibrate with ferrocene as a reference.

**Device Fabrication.** Preliminary EL devices were fabricated with a configuration of ITO/PEDOT:PSS (40 nm)/$CP_n$ (40 nm)/BCP (20 nm)/$Alq_3$ (30 nm)/LiF (1 nm)/Al (100 nm), and encapsulation was performed under a nitrogen atmosphere. The hole injecting PEDOT:PSS layer was spin-coated onto UV-$O_3$-treated indium tin oxide (ITO) substrates and baked at 140 °C for 30 min. Then polymer layer was spin-coated and baked. The thickness of each layer was measured by an ellipsometer. Finally, hole blocking bathocuproine (BCP), electron transporting aluminum(III) tris(8-hydroxyquinolinate) ($Alq_3$), and LiF/aluminum were successively deposited under a base pressure of $<10^{-7}$ Torr. The active area was 2 mm × 2 mm. Current−voltage−luminance characteristics of devices were obtained using a Keithley 237 source measurement unit and a calibrated silicon photodiode connected to an optical powermeter (Newport, 1835C). Electroluminescence spectra were recorded with an Ocean Optics USB2000 fiber-optic spectrometer.

## Results and Discussion

**Synthesis and Characterization of Polymers.** The polymerization procedure and chemical structures of $CP_n$ polymers are shown in Chart 1. To minimize cofacial overlap of carbazole units along the polymer chain, the 3-position of carbazole ring was selected as the anchoring site to the polymer backbone, as shown in Scheme 1.

Vilsmeyer reaction with $POCl_3$ and DMF on a N-alkylated carbazole gave the formylated adduct in good yield. Subsequently, via Wittig olefination with excess potassium carbonate and methyltriphenylphosphonium bromide we could obtain the monomer for hosting part **4**. In the synthesis of ligand-containing monomer **8**, we utilized bromination and Stille reaction (see Scheme 2) because the initial attempt of Vilsmeyer formylation followed by Wittig olefination (see Scheme 1) gave a side product as a major one. Methyl hydroxypicolinate, the protected ancillary ligand, was substituted to another end of dodecyl group in carbazole (**6**) with potassium hydroxide under tempered conditions (50 °C). Then, tetrakis(triphenylphosphine)palladium-(0)-mediated Stille coupling gave the vinylated carbazole product in moderate yield (32%). Subsequent hydrolysis and chelation with the $\mu$-chloride-bridged iridium(III) dimers ($[(dfppy)_2Ir(\mu\text{-}Cl)]_2$) were successfully carried out in dark conditions. The chelation proceeded so fast that blue phosphorescence appeared immediately after the addition of 2 N NaOH to the reaction mixture. The final monomer with FIrpic pendant (**1**) was thoroughly purified via silica column chromatography and identified with $^1H$ NMR, elemental analysis, and high-resolution mass spectrometer.

**Scheme 2. Synthesis of FIrpicDodCbz (1)**

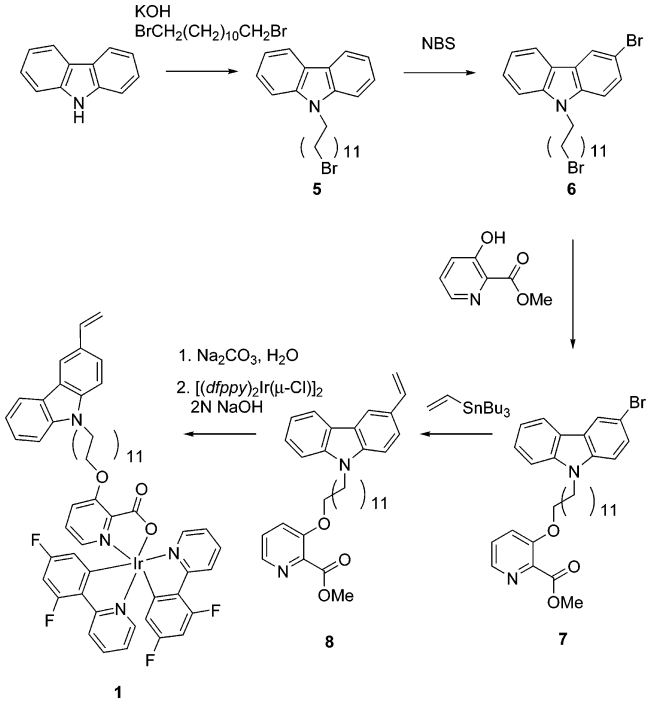


To optimize the composition for complete energy transfer and phase homogeneity, the feed ratio of monomers in the polymer was varied from 1.0 to 15 mol % of FIrpic part (see Table 1). All the synthesized polymers, $CP_n$, showed very good solubility in halogenated solvents such as chloroform, dichloromethane, 1,2-dichloroethane, and monochlorobenzene and showed poor solubility in protic solvents. The comonomer composition, molecular weight, and glass transition temperature ($T_g$) of polymers are summarized in Table 1. Comonomer composition did not exert any distinct effect on the molecular weight and $T_g$ probably because the FIrpic pendants were largely decoupled from the polymer backbone via a dodecyl group. Molecular weights were roughly over 20 000, and glass transition temperatures were around 95 °C.

Determination of comonomer composition in the copolymers was performed with the characteristic band of absorption spectrum of each copolymer. Molar absorption coefficients of 347 nm centered peak of $CP_0$ and 378 nm centered peak of FIrpic were measured and calculated. From the absorption spectra of $CP_n$ in the same weight percent solution ($10^{-4}$ g/mL)

**Table 1. Characterization of $CP_n$ Polymers**

| | monomer feed ratio ($x$:$y$)[a] | comonomer composition ($x$:$y$), $x/(x+y)$ (%) | $M_n$ | $M_w$ | PDI | $T_g$ (°C) |
|---|---|---|---|---|---|---|
| $CP_0$ | (0:100) | (0:100), 0 | 18 000 | 33 100 | 1.84 | 90 |
| $CP_1$ | (1:99) | (1:122), 0.8 | 26 400 | 57 800 | 2.19 | 95 |
| $CP_2$ | (1:32) | (1:34), 2.9 | 21 700 | 50 800 | 2.34 | 99 |
| $CP_3$ | (1:9.0) | (1:18), 5.3 | 33 700 | 65 400 | 1.94 | 97 |
| $CP_4$ | (1:5.7) | (1:8.4), 10.6 | 19 200 | 45 600 | 2.38 | 95 |

[a] See Chart 1 for $x$ and $y$ designations.

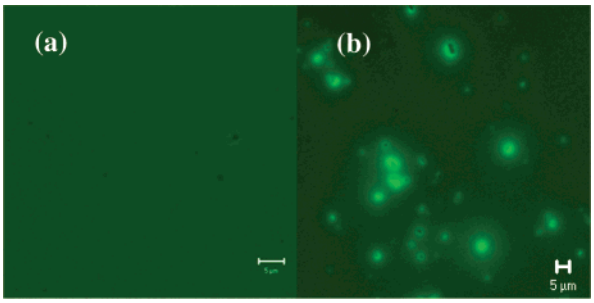


**Figure 1.** Confocal laser scanning microscope images of spin-coated $CP_4$ film on glass (a) and $CP_0$ film doped by FIrpic at the same mole percent of $CP_4$ (10.6%) on glass (b).

in 1,2-dichloroethane, 347 and 378 nm centered Gaussian curves were deconvoluted. The integrated area of each deconvoluted curves were divided by their calibrated molar absorption coefficients, which yielded the corresponding comonomer composition. This procedure was further checked for the simple mixture of $CP_0$ and FIrpic solution in 1,2-dichloroethane for accuracy. As seen in Table 1, comonomer composition for the FIrpic part incorporated to the polymer was slightly less than that initially fed to reaction mixture due to the different reactivity ratios of monomers.

Compared with $CP_0$ film doped by FIrpic, films of $CP_n$ show suppressed heterophasic domain formation. Under the confocal laser scanning microscope, apparent FIrpic aggregates were clearly seen in the case of molecular composites, as shown in Figure 1b. Many spots with bright luminescence are dispersed randomly, which most likely behave as the low-energy traps upon optical or electrical excitation as well as channels for leakage current. It was clearly noted that all the $CP_n$'s are free from this phase separation because the FIrpic groups are covalently tethered to the polymer chain.

**Optical Properties.** PVK and other carbazole-based polymers show intense excimer emission at around 427 nm even in solution compared to the isolated carbazole emission at 360 nm.[18] The excimers behave as the exciton quenching sites which lower the energy transfer efficiency to the guest molecules due to their lower energy level.[19] As seen in Figure 2, the photoluminescence spectrum of $CP_0$ solution shows monomeric carbazole emission centered at 360 nm and weakly bound excimer emission at 378 nm.[18] In the case of PVK, however, the photoluminescence spectrum of solution shows no monomeric emission of cabazole at all. From this, it is importantly noted that $CP_0$ has less excited-state inter-carbazole interactions than PVK due to the less favorable steric interactions.

Another noteworthy point in Figure 2a is the feasibility of Förster energy transfer from host to FIrpic. Because the probability of Förster energy transfer depends on spectral overlap integral between donor emission band and acceptor absorption band, the considerable overlap between MLCT absorption band of FIrpic and emission band of $CP_0$ is likely to guarantee efficient Förster energy transfer from $CP_0$ to FIrpic.[20] Actually, when $CP_0$ film doped with FIrpic was optically excited at the $CP_0$ absorption region, significantly enhanced blue emission of

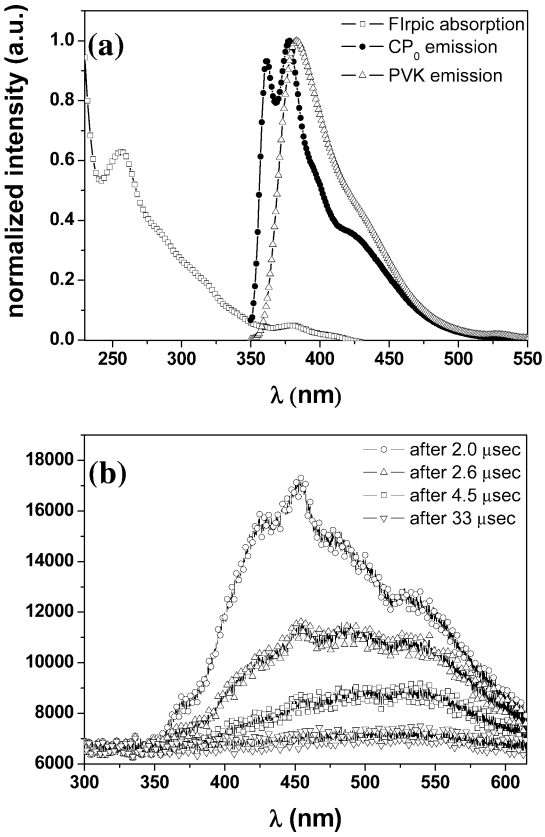


**Figure 2.** (a) Normalized absorption spectrum of FIrpic solution and photoluminescence spectra of $CP_0$ solution and PVK solution in $CH_2Cl_2$. (b) Low-temperature (7 K) time-resolved photoluminescence spectra of spin-coated $CP_0$ film on glass with different delay times.

FIrpic was observed. This Förster energy transfer was more efficiently implemented in $CP_n$ likewise. In $CP_1$, the emission band of backbone $CP_0$ and characteristic FIrpic emission were observed simultaneously, however, with increasing composition of the FIrpic part emission band of $CP_0$ decreased quickly. Even at the low composition of FIrpic ($CP_2$, 2.9%) complete energy transfer from host to FIrpic was effected, as shown in Figure 3b.

Not only the spectral overlap but also the individual energy level matching between host and guest are crucial in the performance of electroluminescence device. It is well-known that the singlet ($S_1$) and triplet excited state ($T_1$) levels of host must lie higher than those of guest to improve the efficiency of triplet−triplet energy transfer.[20] Moreover, hole trapping in the guest and subsequent recombination with electron injected from the metal electrode requires higher oxidation potential of host than guest. Within the limit of energy level of host described above, electrically generated excitons on host which is delivered to guest as well as directly created excitons on guest are able to be confined in the guest without being back-transferred to the host. In this regard, determination of energy level of host is necessary to explain the phenomena related to the energy transfer.

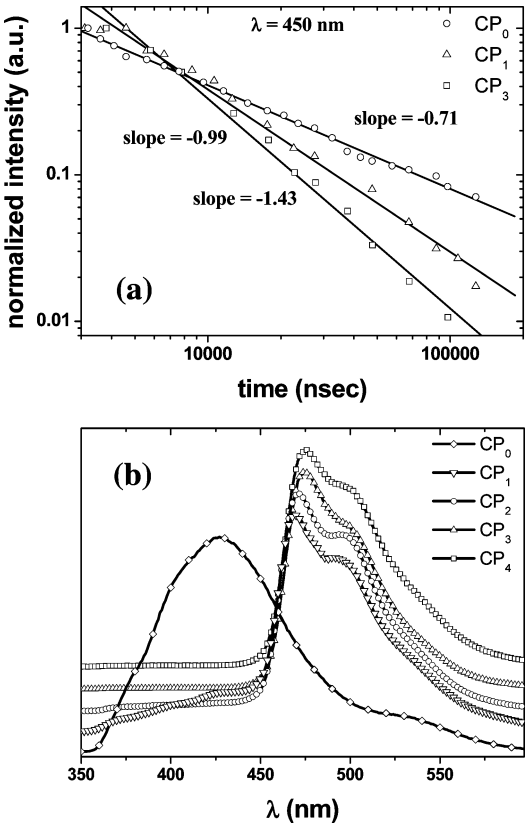


**Figure 3.** (a) Comparison of decay of 450 nm centered time-resolved low-temperature photoluminescence intensity of $CP_3$, $CP_1$, and $CP_0$. (b) Photoluminescence spectra of spin-coated $CP_n$ films on glass; the spectra were shifted vertically for convenience.

The energy gap between $S_1$ and $S_0$ of the host part was calculated as 3.5 eV from the absorption edge of $CP_0$. With the oxidation potential of $CP_0$ determined to be −5.7 eV by cyclic voltametry, the $S_1$ energy level was identified as −2.2 eV relative to vacuum. The position of $T_1$ of $CP_0$ was found by delayed photoluminescence spectra extracted from the low-temperature time-resolved photoluminescence shown in Figure 2b. Apparently, four peaks (424, 450, 485, and 533 nm) were identified from the delayed photoluminescence spectra. Different spectral position of them from room temperature photoluminescence spectra and their longer decay times in microsecond range clearly indicated that they were originated from $T_1$. The higher energy sideband at 370 nm which was also shown at room temperature static photoluminescence was recognized as delayed fluorescence. For the 424 nm photoluminescence peak, however, we could observe the trace of the peak even after 33 $\mu$s. The analysis was rather ambiguous that we could not decide the exact nature of this 424 nm peak, since spectral position coincided with excimer band of $CP_0$. However, the peak position matched that of free triplet exciton reported earlier in the phophorescene spectra of PVK solution.[21]

Because of the low intensity of phosphorescence spectra, peaks after milliseconds were overlaid with noise. The decay dynamics of 450, 485, and 533 nm peak revealed that the lifetimes of them were 13, 15, and 16 $\mu$s, respectively. The position of the first peak (450 nm) in the phosphorescence spectrum of $CP_0$ was located at the higher energy region than that (502 nm) of PVK.[10] As for the fluorescence case explained above, this was attributed to the reduced interchromophoric interactions in $CP_0$. With the first peak of phosphorescence spectra of 450 nm, the $T_1$ energy level was found as −2.6 eV, which is higher than that (−3.1 eV) of FIrpic. So we could expect exothermic triplet−triplet energy transfer from hosting $CP_0$ to FIrpic in this regard.

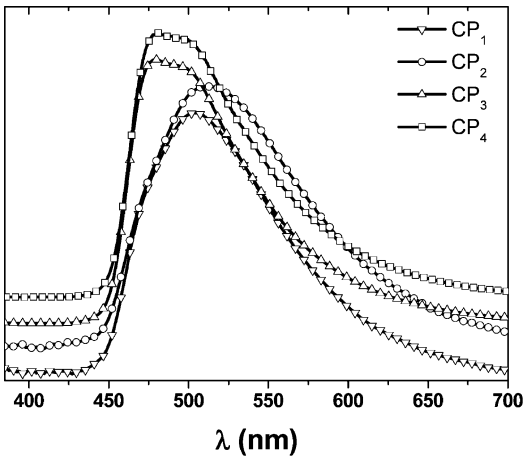


**Figure 4.** Electroluminescence spectra of $CP_n$ at 10 mA/cm$^2$ each. Device structure was ITO/PEDOT:PSS (40 nm)/$CP_n$ (40 nm)/BCP(20 nm)/$Alq_3$ (30 nm)/LiF (1 nm)/Al (100 nm); the spectra were shifted vertically for convenience.

Triplet−triplet energy transfer from hosting part to FIrpic was validated by transient decay centered at 450 nm phosphorescence emission of hosting part. As shown in Figure 3a, decay of triplet excitons in $CP_1$ and $CP_3$ was faster than that in $CP_0$, which indicates additional fast decaying channel for triplet excitons (450 nm) that existed in $CP_1$ and $CP_3$. Considering FIrpic emission of $CP_1$ and $CP_3$ (see Figure 3b), the identity of this channel was safely regarded as triplet−triplet energy transfer from hosting part to FIrpic.

**Electroluminescence Characteristics.** Different from the photoluminescence spectra shown in Figure 3b, we could not find any trace of emission from carbazole backbone in the electroluminescence spectra of $CP_n$, as shown in Figure 4. Even the very low FIrpic content of $CP_1$ (0.8 mol %) ensures complete disappearance of emission from hosting part. Regarding photoluminescence spectra of $CP_1$ showing the backbone emission, the main pathway responsible for emitting state in FIrpic is thought to be direct exciton formation in FIrpic. This reflects effective exciton confinement in the FIrpic unit, which was due to the condition provided by high $T_1$ and low $S_0$ level of hosting part.[22]

Preliminary EL devices incorporating $CP_n$ polymers showed somewhat moderate performance compared with previous report.[6] As summarized in Table 2, peak luminance under 100 mA/cm$^2$ was 1450 cd/m$^2$ for $CP_4$, and maximum emission efficiency at 10 mA/cm$^2$ was recorded 2.23 cd/A for $CP_4$.[23] Luminance as a function of FIrpic composition is shown in Figure 5, and we could observe that higher content of FIrpic part gave better luminance characteristics.

Luminance under 100 mA/cm$^2$ was enhanced 27 times for $CP_4$ (1450 cd/m$^2$) compared to $CP_1$ (54 cd/m$^2$). By varying molar composition of FIrpic part on copolymer from $CP_1$ (0.8%) to $CP_4$ (10.6%), emission efficiency was increased 20 times. Because FIrpic also behaves as charge (probably electron) carrier in the emitting layer, increased content of FIrpic might give better emission efficiency. However, a reference device of doped analogue of $CP_4$ (DP) demonstrated so poor current characteristics that 36 V was required to reach 100 mA/cm$^2$. This is a noteworthy point to show poor current characteristics induced by phase separation in the doped system. Highly aggregated FIrpic (see Figure 1) is prone to act as an obstruction in transporting charge carrier.

**Table 2. Electroluminescent Characteristics of $CP_n$ and DP[a]**

| | $\lambda_{max}$ (nm) | CIE ($x$, $y$) | $V_{turn-on}$ (V) | $V_{drive}$ (V) 10 mA/cm$^2$ 100 mA/cm$^2$ | luminance (cd/m$^2$) 10 mA/cm$^2$ 100 mA/cm$^2$ | emission efficiency (cd/A) 10 mA/cm$^2$ 100 mA/cm$^2$ |
|---|---|---|---|---|---|---|
| $CP_1$ | 500 | (0.26, 0.47) | 5.2 | 12.4 | 14 | 0.15 |
| | | | | 15.6 | 54 | 0.11 |
| $CP_2$ | 500 | (0.30, 0.48) | 4.4 | 9.6 | 19 | 0.19 |
| | | | | 14.0 | 60 | 0.06 |
| $CP_3$ | 474, 500 | (0.24, 0.43) | 5.2 | 12.4 | 120 | 1.08 |
| | | | | 17.8 | 750 | 0.78 |
| $CP_4$ | 474, 500 | (0.23, 0.43) | 5.2 | 10.8 | 220 | 2.23 |
| | | | | 14.4 | 1450 | 1.49 |
| DP | 480, 505 | (0.25, 0.45) | 5.5 | 17.5 | 188 | 1.88 |
| | | | | 36.0 | 1190 | 1.19 |

[a] See text for designations.

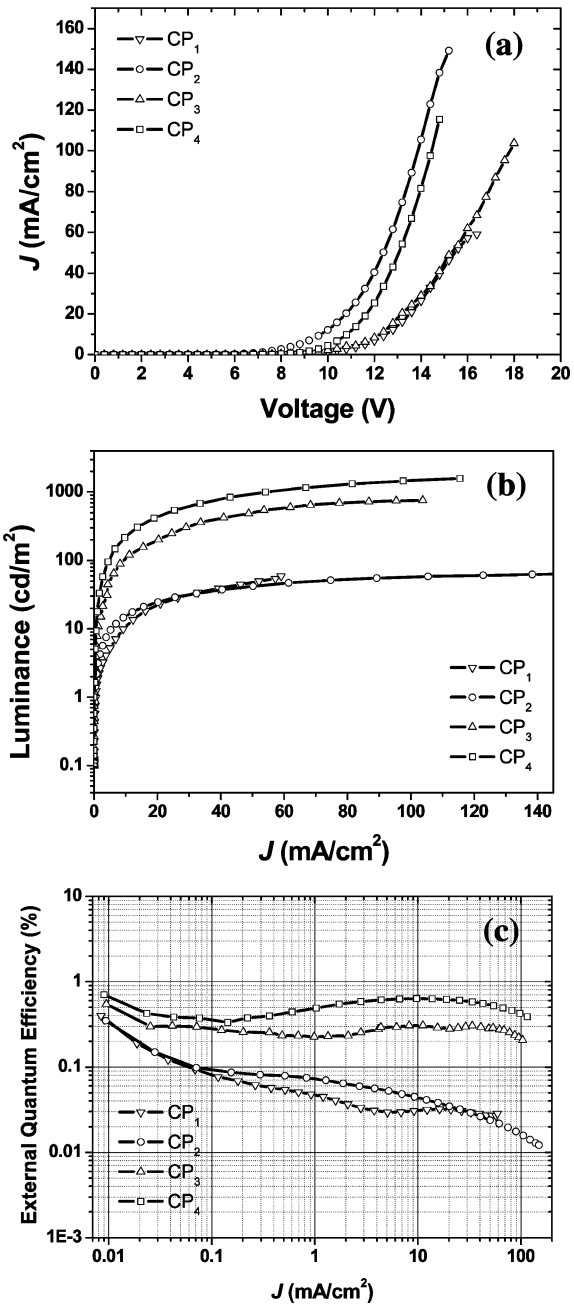


**Figure 5.** (a) Current density vs voltage characteristics of $CP_n$ and their (b) luminance and (c) external quantum efficiency upon current density change.

For $CP_3$ and $CP_4$, maximum external quantum efficiency was observed around 10 mA/cm$^2$ and did not show abrupt decrease to 100 mA/cm$^2$. This suppressed roll-off characteristics of external quantum efficiency in the region of high current density are an encouraging result compared to the doped FIrpic/PVK system.[6] As mentioned before (vide infra), this phenomenon implies less interchromophoric interaction under electrical excitation due to covalently bonded FIrpic to polymer backbone. Well-dispersed triplet emitters, FIrpic, in the host seem to have fewer chances to combine each other to activate a destructive nonradiative pathway.

Even though covalent attachment of FIrpic to the polymer backbone gave suppressed microscale heterophasic formation (see Figure 1), the long dodecyl chain employed in the polymer structure could not prevent nanoscale aggregation in the high contents of FIrpic. From this point of view, our moderate device efficiency is envisaged on the basis of nanometric interchromophoric aggregation which could be possibly reduced by utilizing stiff structure in a future work. Furthermore, well-balanced charge-transport character of host would give rise to improved device efficiency.

## Conclusions

In summary, we have designed and synthesized carbazole-based copolymer tethering blue emitting FIrpic via covalent bond ($CP_n$). Expected suppression of phase segregation compared to the doped analogue was realized and identified by CLSM. By changing anchoring position of carbazole along the polymer chain, minimized excimer formation compared to conventional PVK was achieved. This minimized excited-state interaction in $CP_0$ provided higher $T_1$ level than PVK, through which exothermic triplet−triplet energy transfer to FIrpic as well as Förster transfer could take place. In the electroluminescence device, emission efficiency in the region of 10−100 mA/cm$^2$ showed suppressed roll-off characteristics.

**Acknowledgment.** This work was supported by the Ministry of Science and Technology of Korea through National Research Laboratory (NRL) program awarded to Prof. Soo Young Park. We are grateful for the instrumental support from the equipment facility of CRM-KOSEF, Korea University, and the financial support by Dongwoo FineChem Co., Ltd.

## References and Notes

(1) Adachi, C.; Baldo, M. A.; Thompson, M. E.; Forrest, S. R. *J. Appl. Phys.* **2001**, *90*, 5048.
(2) Baldo, M. A.; O'Brien, D. F.; You, Y.; Shoustikov, A.; Sibley, S.; Thompson, M. E.; Forrest, S. R. *Nature (London)* **1998**, *395*, 151.
(3) Baldo, M. A.; Adachi, C.; Forrest, S. R. *Phys. Rev. B* **2000**, *62*, 10967.
(4) Tokito, S.; Iijima, T.; Suzuri, Y.; Kita, H.; Tsuzuki, Y.; Sato, F. *Appl. Phys. Lett.* **2003**, *83*, 569.
(5) Ren, X.; Li, J.; Holmes, R. J.; Djurovich, P. I.; Forrest, S. R.; Thompson, M. E. *Chem. Mater.* **2004**, *16*, 4743.
(6) Kawamura, Y.; Shozo, Y.; Forrest, S. R. *J. Appl. Phys.* **2002**, *92*, 87.

(7) Negres, R. A.; Gong, X.; Ostrowski, J. C.; Bazan, G. C.; Moses, D.; Heeger, A. J. *Phys. Rev. B* **2003**, *68*, 115209.
(8) Lamansky, S.; Kwong, R. C.; Nugent, M.; Djurovich, P. I.; Thompson, M. E. *Org. Electron.* **2001**, *2*, 53.
(9) Vaeth, K. M.; Tang, C. W. *J. Appl. Phys.* **2002**, *92*, 3447.
(10) Noh, Y.-Y.; Lee, C.-L.; Kim, J.-J. *J. Chem. Phys.* **2003**, *118*, 2853.
(11) Chen, X.; Liao, J.; Liang, Y.; Ahmed, M. O.; Tseng, H.-E.; Chen, S.-A. *J. Am. Chem. Soc.* **2003**, *125*, 636.
(12) Sandee, A. J.; Williams, C. K.; Evans, N. R.; Davies, J. E.; Boothby, C. E.; Köhler, A.; Friend, R. H.; Holmes, A. B. *J. Am. Chem. Soc.* **2004**, *126*, 7041.
(13) Sudhakar, M.; Djurovich, P. I.; Hogen-Esch, T. E.; Thompson, M. E. *J. Am. Chem. Soc.* **2003**, *125*, 7796.
(14) Kim, N.; Webber, S. E. *Macromolecules* **1985**, *18*, 741.
(15) Burkhart, R. D. *Macromolecules* **1976**, *9*, 234.
(16) Burkhart, R. D. *Macromolecules* **1979**, *12*, 1073.
(17) Tokito, S.; Suzuki, M.; Sato, F.; Kamachi, M.; Shirane, K. *Org. Electron.* **2003**, *4*, 105.
(18) Johnson, G. E. *J. Chem. Phys.* **1975**, *62*, 4697.
(19) Vekikouas, G. E.; Powell, R. C. *Chem. Phys. Lett.* **1974**, *34*, 601.
(20) Turro, N. J. *Modern Molecular Photochemistry*; University Science Books; Sausalito, 1991; Chapter 9.
(21) Yokotama, M.; Tamamura, T.; Nakano, T.; Mikawa, H. *J. Chem. Phys.* **1976**, *65*, 272.
(22) Interestingly enough, the electroluminescence spectrum of each device utilizing $CP_n$ showed disturbed shape compared to previous reports and photoluminescence spectra.[6] Their dependent Commission Internationale de L'Eclairage (CIE) coordinates of CP series were changed from CP4 (0.23, 0.43) to CP2 (0.30, 0.48). This unusual phenomenon was also observed as increasing applied voltage. Since emission maximum of $Alq_3$ was observed at 530 nm, we excluded a possibility of exciton migration into the $Alq_3$ layer.
(23) According to previous experiments with FIrpic (10 wt %)/PVK multilayer EL device by Forrest in Princeton University, 0.96% of external quantum efficiency at 100 $mA/cm^2$ was reported. Since the configuration of EL device in our system was not fully optimized, proper selection of hole-block layer and determination of thickness of polymer layer could give better results.

MA052015T